ELSEVIER

Journal of Magnetism and Magnetic Materials 219 (2000) 186–198

and magnetic materials

www.elsevier.com/locate/jmmm

Preparation, magnetic properties and microstructure of lean rare-earth permanent magnetic materials

J. Bernardi[a,*], T. Schrefl[a], J. Fidler[a], Th. Rijks[b], K. de Kort[b], V. Archambault[c], D. Péré[c], S. David[d], D. Givord[d], J.F. O'Sullivan[e], P.A.I. Smith[e], J.M.D. Coey[e], U. Czernik[f], M. Grönefeld[f]

[a]*Institut für Angewandte und Technische Physik, Vienna University of Technology, Wiedner Hauptstr. 8-10, A-1040 Wien, Austria*
[b]*Philips Research, Building WA12, Prof. Holstaan 4, NL 5656 AA Eindhoven, The Netherlands*
[c]*Rhodia Recherches, Centre de Recherches d'Aubervilliers 52, Rue de la Haie Coq, F-93308 Aubervilliers, France*
[d]*CNRS, Laboratoire Louis Néel, 25 Auvenue des Martyrs, B.P. 160, F-38000 Grenoble, France*
[e]*Department of Physics, Trinity College, Dublin 2, Ireland*
[f]*Magnetfabrik Bonn, Dortheenstraße 215, P.B. 2005, D-52010 Bonn, Germany*

Received 22 November 1999; received in revised form 26 May 2000

In memory of Kees de Kort

Abstract

Nanocrystalline, lean rare-earth composite alloys around the nominal composition $Nd_{3.25}Tb_1Fe_{72.75}Co_5B_{18}$ were prepared by various techniques, such as melt-spinning, melt-extraction, splat cooling and mechanically alloying. The Tb and Co content have been found to be crucial in these alloys for achieving high coercivities, up to 500 kA/m. A typical value for the remanence is 1.05–1.10 T. No crystallographic texture was observed, thus, the remanence enhancement was obtained by the spring magnet behavior. The best results have been found when using amorphous precursors and fairly high heating rates during the annealing treatment in an infrared furnace. The amount of Tb could be reduced which yields a lower coercivity but a higher remanence was obtained. TEM and Mössbauer analysis was carried out to determine the volume fraction of soft and hard phases. Optimized magnets contained typically a homogeneous nanocrystalline microstructure of about 50 vol% hard magnetic phase and about 50 vol% soft magnetic α-Fe plus $(Fe,Co)_3B$ with a narrow grain size distribution. The addition of Si or Nb and Cu improved the microstructure and the magnetic properties. Bonded magnets produced from optimized lean rare-earth magnetic powders show an improved corrosion resistance compared to magnets with higher rare-earth content.

PACS: 61.16.Bg; 61.10.Eq; 61.18.Fs; 75.50.Ww; 81.05.Ys; 81.40. − z

Keywords: Lean rare-earth magnetic materials; Remanence enhanced materials; Microstructure; Nanocomposites; Rapid thermal annealing; Hard magnetic RE–Fe-based alloys

* Corresponding author. Tel.: + 43-1-58801-13730; fax: + 43-1-58801-13798.
E-mail address: bernardi@email.tuwien.ac.at (J. Bernardi).

0304-8853/00/$ - see front matter
PII: S0304-8853(00)00435-2

1. Introduction

In the field of permanent magnets there is a need for materials with magnetic properties between those of low-cost ferrites and high-cost, high-performance Nd–Fe–B sintered magnets. It is expected that such a magnet would find several applications in the computer peripherals, automobile and consumer electronics industries. Bonded magnets made of melt spun Nd–Fe–B ribbons are already used for such applications. These materials consist mainly of the hard magnetic $Nd_2Fe_{14}B$ phase, and a significant proportion of the cost of the magnets arises from their high rare-earth content of 12–14 at%. Coehoorn et al. investigated a lean rare-earth nanocomposite magnetic material with the composition $Nd_{4.5}Fe_{77.5}B_{18}$ [1]. The amorphous ribbons were produced by melt-spinning, which then were annealed to give a nanocrystalline mixture of about 50 vol% hard magnetic $Nd_2Fe_{14}B$ and 50 vol% of soft magnetic phases, mainly Fe_3B. The alloy shows a typical large remanence J_r of 1.2 T although the coercive field ${}_iH_c$ of 250–300 kA/m is too low for most applications. The large remanence observed in isotropic lean rare-earth magnetic materials is caused by exchange coupling between hard and soft magnetic grains. In nanocrystalline materials the magnetization within the soft magnetic grains aligns parallel to the average direction of the magnetization of the neighboring hard magnetic grains [2,3]. This results in a significantly enhanced remanence relative to that expected in an ensemble of non-interacting uncoupled grains according to the Stoner–Wohlfarth model [4]. There are two types of lean rare-earth Nd–Fe–B magnets: those with a low B content of 2–10 at% with α-Fe as the majority soft magnetic phase [5–7] and those with higher B content (15–21 at%), with Fe_3B as the main soft magnetic phase [8]. Common for all remanence enhanced materials is the necessity for a grain size of typically 10–30 nm in order to obtain good magnetic properties [9–14].

Micromagnetic simulations for nanocrystalline exchange-coupled materials have shown that the size of the soft and hard magnetic grains is a critical parameter in obtaining high remanence and maximising coercivity. Ideally the grain size should be no more than twice the domain wall width of the hard magnetic phase [15,16]. Theoretically a coercive field ${}_iH_c$ of 1000–1600 kA/m and a remanence J_r of 1.2–0.8 T should be possible for an exchange-coupled material based on $Nd_2Fe_{14}B$ and Fe_3B/α-Fe. In practice these values have not yet been achieved, mainly due to the nanostructures not being sufficiently fine and homogeneous.

Similar to $Nd_2Fe_{14}B$-type magnets a partial substitution of Nd by the heavy rare-earth elements Tb or Dy can improve the coercive field of lean rare-earth magnets, however, associated with a decrease of the remanence [17]. It has been shown that the magnetic properties of lean rare-earth magnetic materials can be improved by the addition of Co and additives like Ga due to a refinement of the microstructure [18,19]. The substitution of Co and Ga led also to a pronounced enhancement of the coercive field together with a good squareness in Nd–Dy containing alloys [18].

It was further reported that the substitution of Fe by Cr leads to an increase of ${}_iH_c$ due to changes of the crystallization behavior and an optimization of the microstructure [20,21]. The objective of this work was to investigate and develop a lean rare-earth containing magnetic materials with improved coercive field without the substitution of Cr.

2. Experimental

The general composition of the lean rare-earth (RE) containing alloys investigated was: $RE_x(Fe_{1-t}Co_t)_{100-x-y-z}B_yA_z$. The RE and the B content was in the range $3 < x < 5.5$ and $15 < y < 25$, respectively. The main RE element used was Nd. In order to increase the anisotropy of the hard magnetic phase up to 30% of the Nd was substituted with Tb. Fe was partly replaced by Co ($0 < t < 0.3$) to improve the coercive field. In addition, minor amounts of additives (A = Ga, Nb, Al, Si, Cu) were used to attempt to refine the nanostructure. The alloys were prepared by melt spinning, melt extracting, mechanical alloying and splat-cooling in order to find optimum preparation conditions.

Melt spinning was performed using a copper wheel of 200 mm diameter. About 10 g of the alloy

ingots were loaded in a quartz or ceramic tube (MgO-stabilized ZrO_2), melted by radio-frequency-induced heating and ejected through a nozzle mounted 1 mm above the copper wheel with a low ejection pressure of 100 mbar. The wheel speed was in the range of 30–50 m/s. The samples prepared by this technique showed a thickness of about 15–80 μm. A subsequent annealing at temperatures up to 800°C for 0–80 s, performed in an infrared rapid thermal annealing (RTA) furnace, caused crystallization of hard- and soft-magnetic phases. The typical heating rate used was 25 K/s. Melt extraction led to the formation of powders rather than ribbons. The greatest degree of amorphousness was obtained by melt extraction at a wheel speed of 30 m/s. Higher wheel speeds resulted in a process more similar to atomization than melt spinning. Splat cooling was used to prepare small flakes of typically 0.1 g, with high cooling rates of $> 10^6$ K/s. The splat cooling system consists of a rotating hammer bound to a closing magnetic circuit. The samples are induction melted and levitated by eddy currents just above the hammer. When the current is turned off, the molten sample drops and is trapped by the fast-moving hammer. A planetary ball mill (Fritsch Pulverisette 5) was used for mechanical alloying (MA) . The mill rotates each of four steel pots about its own axis at 540 rpm, located on a diameter of 250 mm on a disc which rotates at 398 rpm. The pots, made of hardened tool steel, were partly filled with 200 g of high-carbon steel balls of diameter of 10 mm, and 20 g of alloy powder. After sealing the pots in an argon atmosphere (O_2, $H_2O < 1$ ppm), milling was carried out for 64 h. The powder was then removed from the pots under an argon atmosphere.

The structure of the samples was investigated by conventional (XRD) and high-angle X-ray diffraction (HAXRD). The microstructure of selected samples was characterized by means of analytical electron microscopy (AEM) and high-resolution electron microscopy (HREM). Phases were identified by electron diffraction (SAD) as well as energy dispersive X-ray spectroscopy (EDX). Mössbauer spectroscopy (^{57}Fe) was carried out at room temperature on powder and ribbon samples, to examine the distribution of Fe atoms amongst the various phases. This enabled a semi-quantitative determination of the phase constitution. The phase transformation of some alloys was investigated by differential thermal analysis (DTA) in order to optimize the annealing temperature. A Perkin Elmer differential scanning calorimeter (DSC) was used to study the crystallization temperatures of the phases formed in the samples.

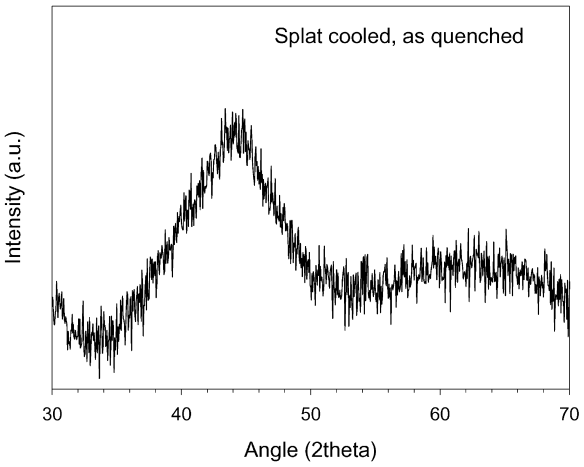

Fig. 1. XRD pattern of an as-prepared splat-cooled sample. Splat cooling usually led to completely amorphous samples after quenching.

Magnetic measurements were performed on flakes of a few milligrams using a vibrating sample magnetometer (VSM). Magnetic fields up to 9 T were applied parallel to the sample plane. Ni-foils with approximately the same shape and orientation as the flakes have been used as calibration samples. Room temperature magnetic properties of splat-cooled flakes were measured using a superconducting-coil 10 T magnetometer. Magnetic properties of mechanically alloyed powders were determined in a novel vibrating sample magnetometer system (VSM) based on a double Halbach permanent magnet arrangement with fields up to 1.1 T. Prior to measurement the powder was mixed with epoxy (Lecoset 7007) in small perspex cylinders and pulsed in an 8 T field to saturate the hard magnetic phase.

Selected alloys were chosen to produce bonded lean rare-earth magnets and to determine their magnetic and mechanical properties. A hydraulic press was used with a maximum force of about 30 t

to produce the resin-bonded samples. The corrosion behavior of bonded magnets has been studied with a NaCl spray test which corresponds to DIN50021-SS standard salt spray test. The magnets were sprayed with a NaCl-solution containing 5 g/100 ml salt for 24 h at a temperature of $35 \pm 2^{\circ}C$ and the properties were determined before and after that test.

3. Results and discussion

3.1. Sample preparation

The different preparation techniques led to a different degree of homogeneity after quenching. Splat cooling, a technique that results in a high cooling rate of the melt, usually produces amorphous flakes with an average thickness of 10–30 μm. Fig. 1 shows a typical XRD pattern of an as prepared splat-cooled sample. The sample does not reveal any sharp diffraction peaks, characteristic of crystalline phases, but rather diffuse peaks associated with an amorphous structure.

Similar results were obtained by melt spinning. The high wheel speed of 30–50 m/s and the low ejection pressure of the melt (about 100 mbar) resulted in the production of thin amorphous ribbons.

Melt extracting led to different results. It was found that the degree of amorphousness depends strongly on the wheel speed and is further influenced by the composition of the melt. This technique produced at high wheel speeds a considerable amount of spherical particles which were fully crystallized and were detrimental to the average magnetic properties of the samples. The formation of spherical particles at high wheel speeds of 40–50 m/s is caused by a process similar to atomization while at a low wheel speed of 30 m/s the process was essentially the same as melt-spinning and produced a high degree of amorphousness. Fig. 2 compares the XRD patterns of as-quenched, melt extracted $Nd_{4.25}Fe_{77.75}B_{18}$ obtained with wheel speeds of 30 and 50 m/s. For a wheel speed of 30 m/s, the flakes are almost amorphous, with minor amounts of α-Fe, Fe_3B and some Fe_2B. Quenching at 50 m/s resulted in less amorphous

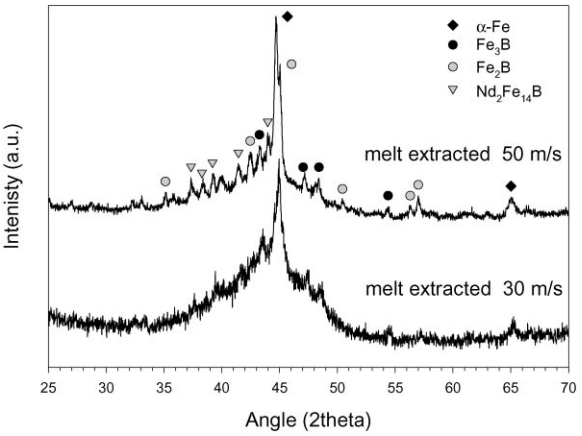

Fig. 2. XRD pattern of melt-extracted $Nd_{4.25}Fe_{77.75}B_{18}$. A higher wheel speed causes the formation of crystallized spherical particles consisting of α-Fe, Fe_3B, Fe_2B and hard magnetic phase.

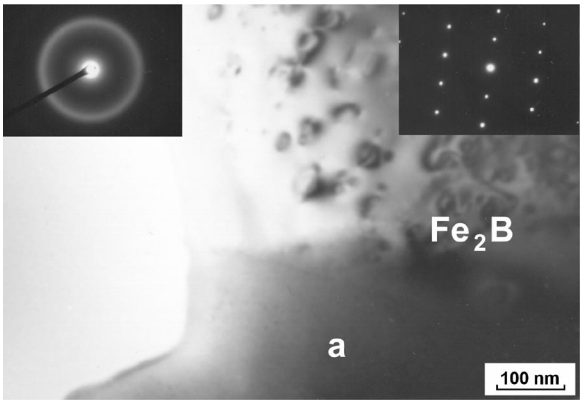

Fig. 3. Electron micrograph and corresponding electron diffraction pattern of a ribbon melt extracted with a wheel speed of 45 m/s showing a large Fe_2B grain embedded within the amorphous RE–Fe–B matrix (a).

phase, with the diffraction lines for α-Fe, Fe_3B, Fe_2B and $Nd_2Fe_{14}B$ clearly visible. These results were also confirmed by electron microscopy (Fig. 3) and Mössbauer spectroscopy. Table 1 summarizes the fractions of phases detected by Mössbauer analysis. It is shown that, in particular, the amount of α-Fe increases with increased wheel speed while the amount of amorphous phase decreases. The reason that there is no significant amount of hard magnetic phase detected in the XRD pattern of the

Table 1
Changes of the phase fractions in $Nd_{4.25}Fe_{77.75}B_{18}$ melt extracted with different wheel speed determined by Mössbauer spectroscopy and comparison of the intrinsic magnetic properties J_s, spontaneous magnetic polarization and A, exchange constant of the main magnetic phases found in the remanence enhanced alloys

Phase	Phase fraction		Anisotropy	J_s (T)	A (pJ/m)
	30 m/s (%)	50 m/s (%)			
Amorphous phase	95	91	—	—	—
$Nd_2Fe_{14}B$	2	3	Uniaxial	1.61	12.5
α-Fe	1	3	Cubic	2.15	25.0
Fe_3B	2	3	In plane	1.62	12.5
$Fe_{23}B_6$	—	—	Cubic	1.70	17.0

sample melt extracted with 30 m/s could be due to fact that the average size of the hard magnetic grains is too small to be seen by XRD.

Mechanical alloying (MA) of rare-earth–transition metal (RE–TM) compounds generally produces materials with a similar structure to those produced by rapid quenching processes and is has been shown that RE–Fe–B alloys produced by annealing mechanically alloyed powders have comparable properties to commercial melt spun alloys [22]. However, the phase formation process in mechanical alloying is different from that of rapid quenching, and the as-milled structures are usually different from the as-quenched structures. Mechanical alloying results typically in either amorphi zation of the compound, or disproportionation of the compound into an amorphous RE–TM phase and a nanocrystalline transition metal solid solution [23]. This is generally true of the lean rare-earth alloys produced in this study. As can be seen in the X-ray diffraction plot for as-milled $Nd_{4.25}Fe_{77.75}B_{18}$ powder shown in Fig. 4, peaks for $Nd_2Fe_{14}B$ that are no longer discernible, and there is severe broadening of the Fe_2B and α-Fe peaks. The mean grain size of the crystalline phases was calculated to be approximately 10 nm, using the Scherrer formula. As-milled powder of all compositions contained an amorphous RE–TM–B phase, TM_2B and a bcc TM solid solution (Fig. 5). In many of the as-milled powders, traces of RE–TM–B intermetallic compounds were found to have persisted during milling. However, for the most part, the intermetallics which had been present in the starting ingot material were amorphized

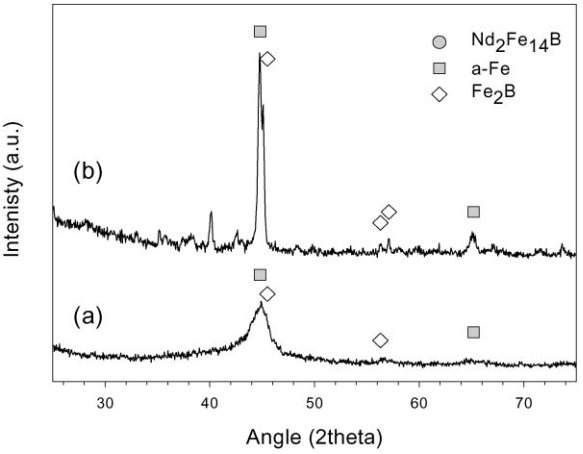

Fig. 4. X-ray diffraction spectra for $Nd_{4.25}Fe_{77.75}B_{18}$ after mechanical alloying (a) and annealing at 690°C for 30 min (b).

or disproportionated to a mixture of an amorphous phase and nanocrystalline phases.

It is important to note that the formation of a multi-phase precursor material prior to annealing is quite different to the situation for rapid quenching techniques like melt spinning or splat cooling, which usually formed a 100% amorphous precursor. Nevertheless, common for the rapid quenching techniques and mechanically alloying is that an annealing treatment is required to crystallize the amorphous phase. Figs. 6 and 7 compare the Mössbauer spectra of a melt spun and annealed lean rare-earth sample and a MA sample with similar composition. While the melt spun sample contains mainly the hard magnetic phase (about 50 vol%) and the $(Fe,Co)_3B$ phase (about 50 vol%), there is

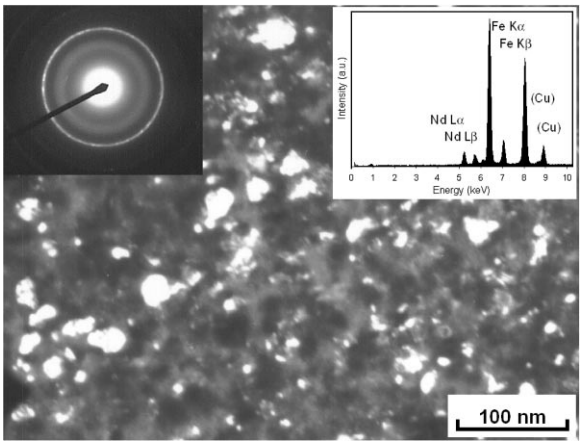

Fig. 5. Dark field electron micrograph of mechanically alloyed $Nd_{4.25}Fe_{77.75}B_{18}$. The corresponding diffraction pattern confirms the formation of α-Fe and Fe_2B that appear as bright grains within the amorphous matrix. Cu in the EDX spectra results from the supporting Cu grid.

a significant amount of $RE_{1.1}Fe_4B_4$ phase found in the mechanically alloyed and annealed powder which reduces the amount of the hard magnetic phase to about 20 vol%. This could be due to pre-existing nuclei of $RE_{1.1}Fe_4B_4$ phase which were not amorphized by MA, as well as a mixture of $(Fe,Co)_2B$ and α-(Fe,Co) that is formed during mechanical alloying. However, the presence of the soft magnetic $(Fe,Co)_2B$ and α-(Fe,Co) phases in MA alloys does not diminish the magnetic properties as long as the grain size of that phases is sufficiently small.

3.2. Coarse selection

In order to investigate the influence of the alloying elements on the magnetic properties a broad range of starting compositions was defined that were produced by the different techniques described above. Each sample was optimally quenched, or mechanically alloyed, then annealed. The general composition of the alloys was: $RE_x(Fe_{1-t}Co_t)_{100-x-y-z}B_yA_z$. The RE (RE = Nd, Tb) and the B content were in the range $3 < x < 5.5$ at% and $15 < y < 25$ at%, respectively. Up to one-hird of Nd was replaced by Tb in some samples in order to increase the anisotropy of the hard magnetic phase. The magnetic moments of Tb couple antiparallel to the transition metal moments and any substitution of Tb is expected to reduce the remanence. Fe was partly replaced by Co ($0 < t < 0.3$). In addition minor amounts of additives (A = Nb, Al) were used in the coarse selection.

During the coarse selection it became evident that a B content of 16.5–23 at% is necessary in order to obtain good magnetic properties. The highest values of coercivity, combined with a high remanence and high $(BH)_{max}$ were found around a B content of 18 at% and a RE content between 3 and 4.25 at% in rapidly quenched alloys. The low amount of hard magnetic phase (about 20 vol%) and the significant formation of 1 : 4 : 4 phase in MA alloys resulted typically in inferior magnetic properties compared to rapidly quenched alloys.

With a high B content of 25 at% neither high remanence nor high coercivity could be obtained. High remanence, but only low coercive fields were measured for alloys with low RE content of 3 at%. Electron microscopy confirmed the formation of large α-Fe grain in samples with low RE content, which decrease the coercive field significantly (Fig. 8). An increasing RE content tends to lead to a reduced remanence and a decrease in remanence enhancement. Alloys with more than 5.5 at% RE exhibit only weak magnetic properties. Phase analysis by HAXRD performed on some of these higher RE containing alloys showed that no $Nd_2Fe_{14}B$ had been formed. Instead, there were large amounts of α-Fe as well as other soft magnetic or paramagnetic phases such as $Nd_2Fe_{23}B_3$, $Nd_{1.1}Fe_4B_4$ and $NdFe_{12}B_6$, which is in agreement with findings of Coehoorn et al. [8].

An exception to this was a mechanically alloyed sample with 5.5 at% Nd that showed a high coercive field of 414 kA/m but, similar to other samples with high RE content, only a low remanence was measured.

Tb substitution was found to have a beneficial effect on the coercive field with only a small decrease in the remanence. This effect is also confirmed by micromagnetic modeling performed for nanocomposite structures, which predicts an increase of the coercive field up to 30% without a significant loss in remanence, as the composition

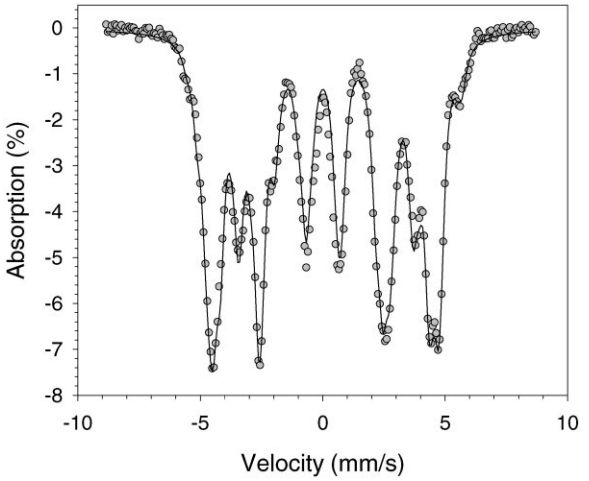

Fig. 6. Mössbauer data and fitted spectrum for melt spun and optimally annealed $Nd_{3.25}Tb_1Fe_{72.75}Co_5B_{18}$.

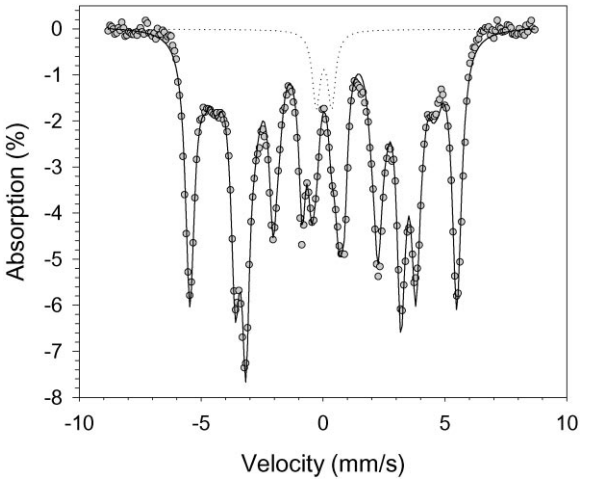

Fig. 7. Mössbauer data and fitted spectrum for mechanically alloyed and annealed $Nd_{3.25}Tb_1Fe_{72.75}Co_5B_{18}$ showing also the fitted paramagnetic subspectrum (dotted line).

of the hard magnetic $Nd_2Fe_{14}B$ phase is changed to $(Nd_{0.75}Tb_{0.25})_2Fe_{14}B$ [24,25]. The partial replacement of Fe by 5 at% Co tends to increase the coercive field and the remanence enhancement but causes a slight decrease of the remanence. A substitution of 15 at% Co usually diminished the magnetic properties drastically. The beneficial effect of a partial Co substitution in lean rare-earth alloys has also been observed by Hirosawa et al. [18].

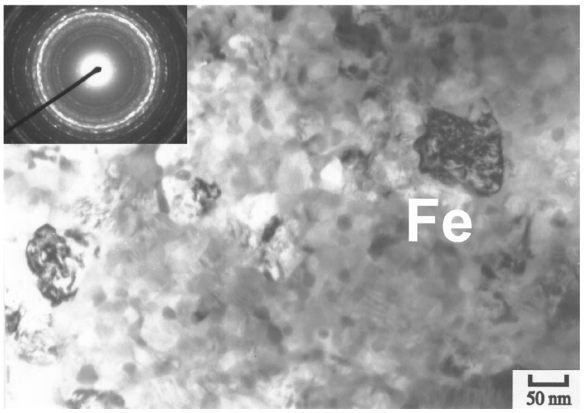

Fig. 8. Microstructure of rapidly quenched and optimally annealed $Nd_3Fe_{79}B_{18}$ showing the presence of large α-Fe grains that diminish the coercive field.

DSC measurements indicate that Co influences the crystallization process of lean rare-earth alloys during annealing (Fig. 9). With Co, a higher transformation rate from the amorphous to the crystalline state is observed which is expressed in sharper DSC peaks in the DSC trace. In addition a lower crystallization temperature of the hard magnetic phase is found (second peak of the DSC trace). The smaller gap between the crystallization temperatures of the hard and soft magnetic phases causes an earlier crystallization of the hard magnetic phase during annealing and could therefore result in a less-promoted grain growth of soft phases and a more homogeneous nanostructure of hard and soft magnetic grains.

The coarse selection led to the identification of some promising compositions that are summarized in Table 2. All that alloys were produced by rapid thermal annealing with a typical heating rates of 20–30 K/s from amorphous precursors. This type of annealing treatment led to better magnetic properties than by conventional annealing with a slow heating rate. Common for that alloys is also that a combination of Co and Tb together with a RE content of about 4.25 at% appears to be crucial in order to obtain high coercive fields.

Samples containing Tb show typically an increased coercive field and a reduction of the saturation magnetization. The substitution of Co for Fe results also in an increase of the coercive field and

a decrease of J_s. In addition the remanence enhancement is improved in Co substituted samples.

High values of the remanence and of the coercive field were found with the composition $Nd_{3.25}Tb_1Fe_{72.75}Co_5B_{18}$, exceeding values for $_iH_c$ reported in the literature [19]. High remanence and a high degree of remanence enhancement were obtained in alloys $Nd_2Tb_1Fe_{73}Co_5Nb_1B_{18}$ and $Nd_3Fe_{73}Co_5Nb_1B_{18}$. Fig. 10 compares the demagnetization curves of $Nd_{3.25}Tb_1Fe_{72.75}Co_5B_{18}$ and $Nd_3Fe_{73}Co_5Nb_1B_{18}$. It is obvious that a higher rare-earth content results in a decrease of the magnetization as well as a significantly increased coercive field.

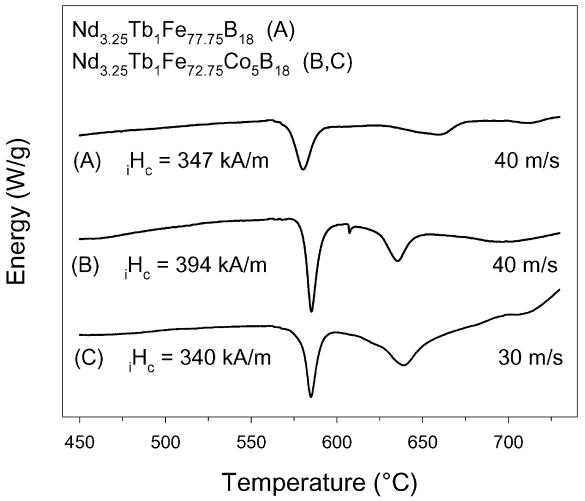

Fig. 9. DSC traces of melt spun $Nd_{3.25}Tb_1Fe_{77.75}B_{18}$ (A) and $Nd_{3.25}Tb_1Fe_{72.75}Co_5B_{18}$ (B, C) measured at a heating rate of 10°C/min. The smaller area of the first crystallization peak of the $Nd_{3.25}Tb_1Fe_{72.75}Co_5B_{18}$ ribbon prepared with 30 m/s indicates a larger amount of soft magnetic grains formed already after quenching compared to the ribbon quenched with 40 m/s. No change of the crystallization behavior and the magnetic properties for different wheel speeds is observed in melt spun $Nd_{3.25}Tb_1Fe_{77.75}B_{18}$.

The change of the magnetic properties detected in the alloys with a RE content of 3 and 4.25 at%, respectively, is also reflected in changes of the phases present in that alloys as shown by X-ray diffraction, Mössbauer spectroscopy as well as selected area electron diffraction. Typically, in alloys with a high RE content (4.25 at%), Fe_3B is found together with the hard magnetic $RE_2Fe_{14}B$ phase (Fig. 11) while alloys with a low RE content (3 at%) consist mainly of $RE_2Fe_{14}B$ and the cubic $Fe_{23}B_6$ phase (Fig. 12). In all samples some α-Fe was detected. Depending on the annealing conditions, traces of Fe_2B could be found in $Nd_{3.25}Tb_1Fe_{72.75}Co_5B_{18}$. Both high remanence samples that showed the formation of $Fe_{23}B_6$ contained Nb as an additive. It is not clear whether the formation of $Fe_{23}B_6$ is caused mainly by the low RE content or also influenced by Nb because $Fe_{23}B_6$ was also found in other alloys with a RE content of 3 at% and no addition of Nb. The increased remanence enhancement found in alloys with low RE content can be attributed to the higher values of the magnetic polarization and the exchange constant of soft magnetic $Fe_{23}B_6$ compared to Fe_3B (see Table 1). Micromagnetic calculations have shown [26] that for nanocrystalline magnetic materials with an average grain size of 20 nm the remanence is increased by replacing Fe_3B by $Fe_{23}B_6$ or α-Fe, respectively, and simultaneously, the coercive field is decreased. Typical for all samples with

Table 2
Composition and room temperature magnetic properties of optimally annealed alloys after the coarse selection (a), of melt spun $Nd_{4.25}Fe_{77.75}B_{18}$ magnets with the addition of Si, Ga or SiNb (b) and of an optimized magnet containing NbCu (c)

Composition	J_r (T)	$_iH_c$ (kA/m)	J_s (T)	J_r/J_s	
$Nd_{3.25}Tb_1Fe_{72.75}Co_5B_{18}$	1.08	394	1.45	0.74	(a)
$Nd_2Tb_1Fe_{73}Co_5Nb_1B_{18}$	1.18	264	1.45	0.81	(a)
$Nd_3Fe_{73}Co_5Nb_1B_{18}$	1.33	206	1.68	0.79	(a)
$Nd_{3.25}Tb_1Fe_{77.75}B_{18}$	1.05	347	1.53	0.69	(a)
$Nd_{4.25}Fe_{77.75}B_{18}$	1.04	238	1.64	0.64	(b)
$Nd_{4.25}Fe_{76.75}Si_1B_{18}$	1.15	275	1.64	0.70	(b)
$Nd_{4.25}Fe_{76.75}Ga_1B_{18}$	1.12	219	1.64	0.68	(b)
$Nd_{4.25}Fe_{76.75}Si_{0.5}Nb_{0.5}B_{18}$	1.06	268	1.55	0.69	(b)
$Nd_{3.25}Tb_1Fe_{71.75}Co_5Cu_{0.5}Nb_{0.5}B_{18}$	1.05	424	1.47	0.71	(c)

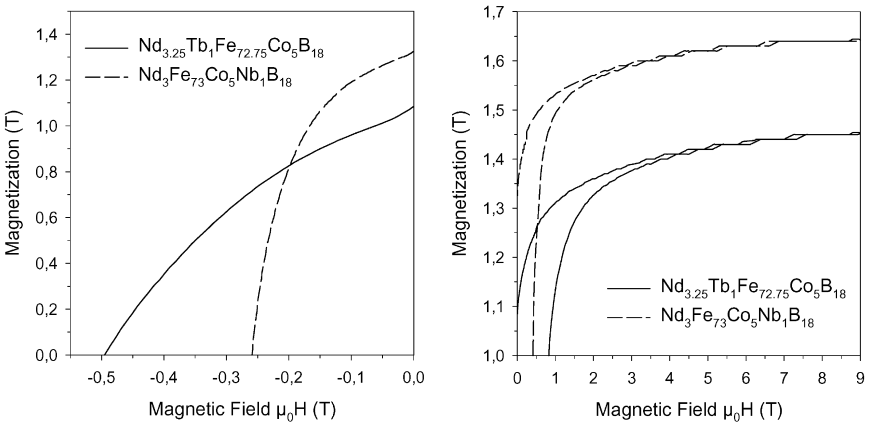

Fig. 10. Demagnetization curves of melt spun and optimally annealed $Nd_{3.25}Tb_1Fe_{72.75}Co_5B_{18}$ and $Nd_3Fe_{73}Co_5Nb_1B_{18}$ in the second and first quadrant of the hysteresis curve. The alloy with 3 at% RE shows a high remanenc enhancement J_r/J_s of 0.79.

optimum magnetic properties is the formation of a homogeneous nanoscale microstructure with an average grain size of 20–40 nm (Fig. 13).

The recoil curves of $Nd_{3.25}Tb_1Fe_{72.75}Co_5B_{18}$ shown in Fig. 14 demonstrate the 'exchange spring' behavior of the magnetization that is typical for exchange-coupled nanocomposite structures consisting of hard and soft magnetic grains. The reversible behavior of the magnetization is observed for magnetic fields up to $0.8\ {}_iH_c$. The small kink at very low fields indicates a small fraction of uncoupled soft magnetic grains.

3.3. Optimization of the preparation conditions

Rapid quenching using a wheel speed of 30–50 m/s usually produced amorphous precursors. Lower wheel speeds generally caused a higher degree of crystallinity in the as-quenched alloys due to the slower cooling rate. The crystallization behavior is influenced by the composition of the alloys, as shown in Fig. 9. While there are no changes in the electron diffraction patterns and HAXRD spectra being observed in a Co containing alloy prepared with a wheel speed of 30–50 m/s, DSC measurements reveal a higher degree of crystallization of the soft magnetic phases in the case of a low wheel speed. This results are in agreement with magnetic measurements which show a reduced coercive field for samples prepared with 30 m/s. No influence of the wheel speed on the

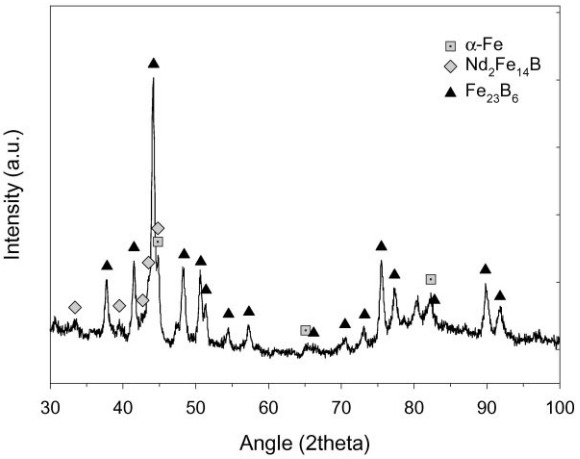

Fig. 11. HAXRD spectrum of optimally annealed alloy $Nd_{3.25}Tb_1Fe_{72.75}Co_5B_{18}$ showing the presence of α-Fe, Fe_3B and $Nd_2Fe_{14}B$.

crystallization behavior and the magnetic properties was observed in a similar sample without Co substitution.

The optimum magnetic properties for rapidly quenched alloys were usually obtained by applying a rapid thermal annealing treatment (RTA) with high heating rates as compared to conventional annealing. This is due to the fact that soft magnetic phases crystallize at lower temperatures than the hard magnetic phase (see Fig. 9). A high heating rate prevents excessive grain growth of soft

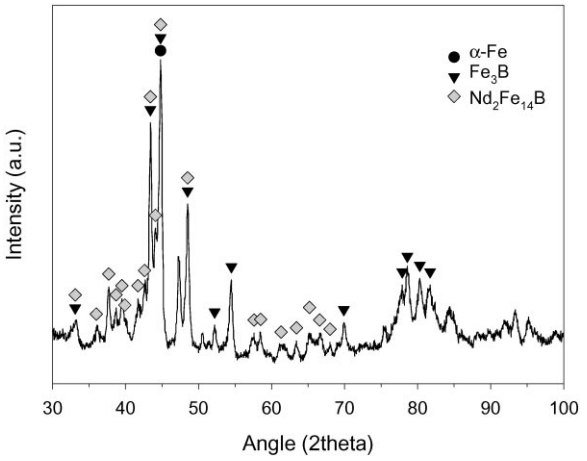

Fig. 12. HAXRD spectrum of optimally annealed alloy $Nd_2Tb_1Fe_{73}Co_5Nb_1B_{18}$ showing the presence of α-Fe, $Fe_{23}B_6$ and $Nd_2Fe_{14}B$.

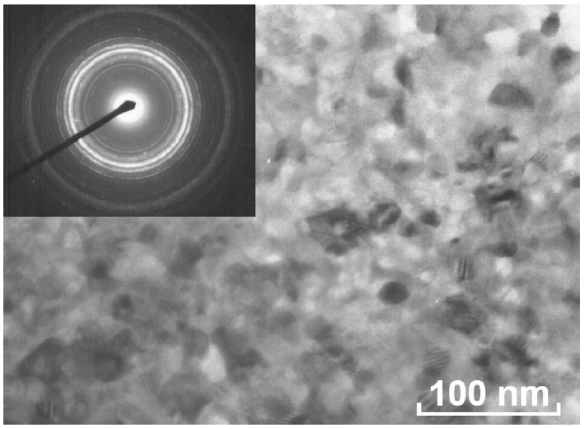

Fig. 13. Electron micrograph and corresponding diffraction pattern showing the typical microstructure of melt spun and optimally annealed $Nd_{3.25}Tb_1Fe_{72.75}Co_5B_{18}$. The diffraction pattern shows diffraction rings from hard magnetic $RE_2Fe_{14}B$ and Fe_3B grains.

magnetic phases before the hard magnetic grains start nucleating and should promote a more balanced nanostructure of hard and soft magnetic grains. To suppress the formation of soft phases the samples were typically annealed with a heating rate of 15–25 K/s up to the annealing temperature of 600–820°C. After a dwell time of about 0–120 s the samples were cooled quickly to room temperature.

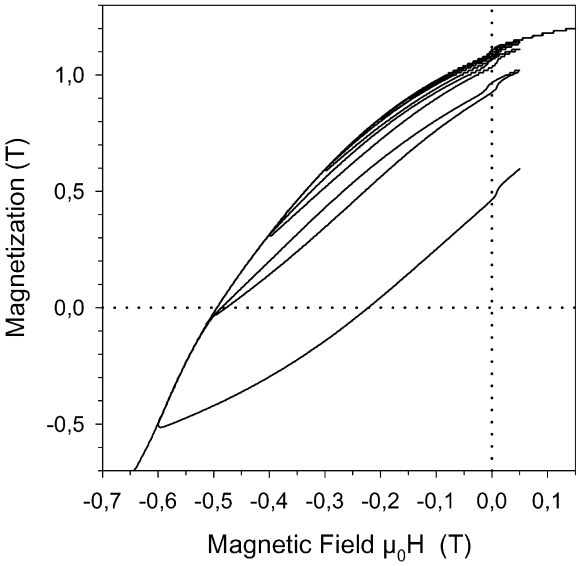

Fig. 14. Recoil curves of $Nd_{3.25}Tb_1Fe_{72.75}Co_5B_{18}$ indicating typical exchange spring behavior observed in nanocrystalline exchange coupled hard and soft magnetic grains. Prior to measurement the sample was saturated at 9 T.

The optimum heating rates as well as the annealing temperatures depend strongly on the composition of the alloys. A high heating rate of about 50 K/s or more usually led to the formation of larger α-Fe grains up to 100 nm throughout the samples and to a deterioration of the magnetic properties. The mechanism responsible for the favored growth of α-Fe is not quite understood yet.

3.4. Optimization of the composition and magnetic properties

Additives are commonly used to improve the magnetic properties and the phase formation in hard and soft magnetic materials [27]. The effect of small amounts of Si, Ga and Nb on the coercive field, due to changes of the nanostructure, has been investigated on the alloy $Nd_{4.25}Fe_{77.75}B_{18}$. While there was no improvement of the magnetic properties found in splat-cooled materials there is a clear indication that Si and Si + Nb improves ${}_iH_c$ as well as the remanence and remanence enhancement in melt spun alloys (Table 2). Ga has only a small effect on the remanence enhancement but reduces the coercive field.

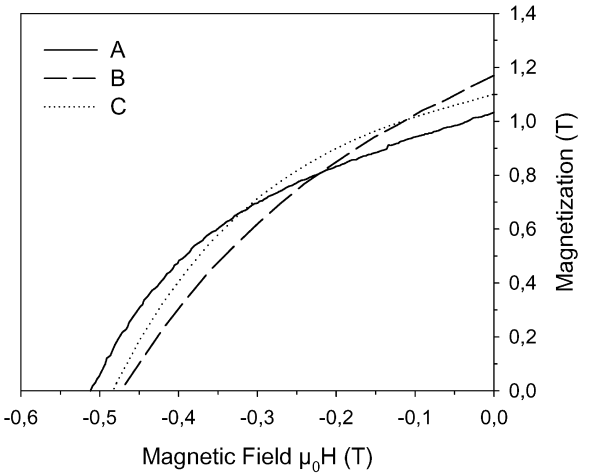

Fig. 15. Demagnetization curves for spalt cooled and flash annealed alloys showing the effect of Co and Si on the remanence and coercive field for (A) $Nd_{3.25}Tb_1Fe_{72.75}Co_5B_{18}$, (B) $Nd_{3.25}Tb_1Fe_{77.75}B_{18}$ and (C) $Nd_{3.25}Tb_1Fe_{71.75}Co_5Si_1B_{18}$.

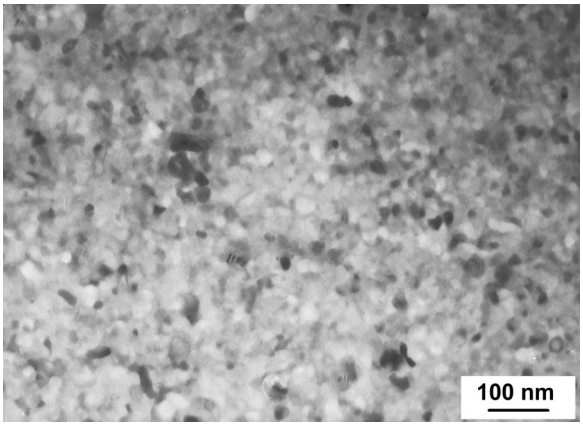

Fig. 16. Electron micrograph of melt extracted and rapid thermal annealed $Nd_{3.25}Tb_1Fe_{71.75}Co_5Cu_{0.5}Nb_{0.5}B_{18}$ showing a homogeneous grain size distribution and an average grain size of about 25 nm.

It has been shown that the combination of Co and Si improves the magnetic properties of nanocrystalline RE–Fe–Cr–B exchange coupled magnets [28]. A similar effect is also found in the investigated alloys that contain no Cr (Fig. 15). It is obvious that the substitution of Co leads to an improvement of ${}_iH_c$ and to a significant decrease of B_r. If a combination of Co and Si is used the remanence and the loop squareness are enhanced significantly and the coercive field is improved slightly. With an increasing amount of Si, the saturation magnetization of the alloys decreased. This effect is not only attributed to changes of the intrinsic properties of the hard magnetic phase but presumably also to changes of the phase constitution due to the formation of silicides. However, XRD as well as electron diffraction did not show that any detectable amount of silicide phases was formed in alloys with higher Si content. Microstructural investigations of melt spun alloys containing Co and Si indicated that an improvement of the magnetic properties was correlated with the formation of a more homogeneous microstructure with a narrow grain size distribution.

Nb and Cu are well-known additives in soft magnetic nanocrystalline materials in order to control the grain size. The addition of NbCu has been also investigated in lean rare-earth alloys. By replacing Fe by 1 at% NbCu the coercive field of melt spun and fast-annealed $Nd_{3.25}Tb_1Fe_{71.75}Co_5Cu_{0.5}Nb_{0.5}B_{18}$ could be increased to 424 kA/m while keeping a high remanence of 1.05 T (see Table 2). The NbCu containing alloys produced by rapid quenching usually contained a very homogeneous microstructure. Optimum magnetic properties were obtained with alloys showing a small average grain size of 15–25 nm (Fig. 16).

DSC measurements have shown that the substitutions of Tb for Nd and Co for Fe lower the crystallization temperature of the hard magnetic phase (T2) in rapid-quenched lean rare-earth alloys while the crystallization temperature of the soft magnetic phase (T1) remains unaltered. A comparison of the crystallization temperatures and the magnetic properties for selected alloys (Table 3) shows that there is a clear correlation between the coercive field and T2. The reduction of the temperature difference between the crystallization temperatures of the hard and soft magnetic phases seems to promote the formation a more homogeneous nanostructure when applying a rapid thermal annealing with a high heating rate. This enables an improved exchange coupling between hard and soft magnetic phases and improves therefore the

Table 3
Crystallization temperatures of the soft (T1) and hard magnetic phase (T2), coercive field ${}_iH_c$ and remanence enhancement J_r/J_s for lean rare-earth alloys. T1 and T2 have been measured in the DSC using a ramp of 20°C/min

Composition	T1 (°C)	T2 (°C)	${}_iH_c$ (kA/m)	J_r/J_s
$Nd_{3.25}Tb_1Fe_{77.75}B_{18}$	579	659	347	0.69
$Nd_{3.25}Tb_1Fe_{72.75}Co_5B_{18}$	585	636	394	0.75
$Nd_{3.25}Tb_1Fe_{71.75}Co_5Cu_{0.5}Nb_{0.5}B_{18}$	588	615	424	0.71

Table 4
Decrease of the physical and magnetic properties of bonded lean rare-earth $Nd_{3.25}Tb_1Fe_{72.75}Co_5B_{18}$ and a magnet with higher rare-earth content after the salt spray test

Composition	Weight (%)	Density (%)	J_r (%)	${}_iH_c$ (%)	BH_{max} (%)
$Nd_{3.25}Tb_1Fe_{72.75}Co_5B_{18}$	− 0.1	0.0	− 2.6	− 1.6	− 5.8
~$Nd_{11.5}Fe_{82.5}B_6$	− 4.3	− 2.2	− 4.2	− 0.9	− 7.4

coercive field. A similar relationship between crystallization temperatures and magnetic properties was also found in the mechanically alloyed samples.

3.5. Application of powders in bonded magnets

Resin-bonded magnets were produced from $Nd_{3.25}Tb_1Fe_{72.75}Co_5B_{18}$ powder. The magnetic properties of that lean rare-earth alloy, measured from ribbons, are $J_r = 1.08\,T$, ${}_iH_c = 400\,kA/m$ and $BH_{max} = 100\,kJ/m^3$. The temperature dependence of the remanence and of the coercive field are $(1/J_r)dJ_r/dT = -0.04\%/K$ and $(1/{}_iH_c)\,d_iH_c/dT = -0.40\%/K$, respectively.

The bonded samples typically consisted of 97.3 wt% magnetic powder, 2.4 wt% resin and 0.3 wt% stearate. The bonded $Nd_{3.25}Tb_1Fe_{72.75}Co_5B_{18}$ magnet showed a remanence $B_r = 0.72\,T$, a coercive field ${}_iH_c = 385\,kA/m$ and $BH_{max} = 52\,kJ/m^3$. The corrosion resistance was determined using a standard salt spray test. The results of this test for the lean rare-earth $Nd_{3.25}Tb_1Fe_{72.75}Co_5B_{18}$ magnet are summarized in Table 4 and compared with those for a bonded magnet with nearly stoichiometric $Nd_2Fe_{14}B$ composition. The lean rare-earth $Nd_{3.25}Tb_1Fe_{72.75}Co_5B_{18}$ magnets appear more corrosion-resistant compared to magnets with a higher rare-earth content.

4. Conclusions

By applying non-equilibrium processing techniques it was possible to produce lean rare-earth remanence enhanced magnetic materials with high remanence and moderately high coercive field. Rapidly quenched materials had better properties than those produced by mechanical alloying, due to incomplete formation of the hard phase in the latter. A fast annealing with a typical heat rate of 15–25°C/s led to better magnetic properties than conventional annealing treatment. The main results are:

- the partial substitution of Tb for Nd together with the substitition of Co for Fe has been found crucial in order to obtain high coercive fields;
- the minimum RE content for high coercive fields is about 4.25 at%;
- alloys with 4.25 at% RE consist typically of hard magnetic $RE_2(Fe,Co)_{14}B$ and soft magnetic $(Fe,Co)_3B$ grains. In alloys with 3 at% RE $Fe_{23}B_6$ is found as the main soft magnetic phase;
- the optimum B content is around 18 at%. A higher or a lower B content results in a deterioration of the magnetic properties;
- the addition of minor amounts of Si improves the remanence as well as the squareness of the demagnetization curve;

- the addition of NbCu improve the coercive field while keeping a high remanence;
- good magnetic properties are found in magnets with a small grain size and a homogeneous microstructure. A coarser grain size and the formation of larger α-Fe grains leads usually to a decrease of the coercive field.

Optimum magnetic properties ($J_r = 1.05\,T$, ${}_iH_c = 424\,kA/m$, $J_r/J_s = 0.71$) were obtained with melt spun and rapid thermal annealed $Nd_{3.25}Tb_1Fe_{71.75}Co_5Cu_{0.5}Nb_{0.5}B_{18}$. The ribbons of this alloy had a homogeneous nanostructure with an average grain size of 15–25 nm. Bonded magnets produced from lean rare-earth alloys appear to be more corrosion resistant compared to alloys with a higher RE content.

Acknowledgements

This work has been supported by EC-BRITE/EURAM Project No. BRPR-CT95-0097.

References

[1] R. Coehoorn, D.B. deMooij, J.P.W.B. Duchateau, K.H.J. Buschow, J. Phys. C 8 (1988) 669.
[2] M.G. Grönefeld, Ph.D.Thesis, University of Stuttgart, Germany, 1990.
[3] E.F. Kneller, R. Hawig, IEEE Trans. Magn. 27 (1991) 3588.
[4] E.C. Stoner, E.P. Wohlfarth, Philos. Trans. Roy. Soc. London Ser. A 240 (1948) 599.
[5] G.C. Hadjipanayis, L. Withanawasam, R.F. Krause, IEEE Trans. Magn. 31 (1995) 3596.
[6] V. Panchanathan, IEEE Trans. Magn. 31 (1995) 3605.
[7] T. Nishio, S. Koyama, Y. Kasai, V. Panchanathan, J. Appl. Phys. 81 (8) (1997) 4447.
[8] R. Coehoorn, D.B. deMooij, C. deWaard, J. Magn. Magn. Mater. 80 (1991) 101.
[9] T. Schrefl, J. Fidler, J. Magn. Magn. Mater. 177–181 (1998) 970.
[10] A. Manaf, M. Al-Khafaji, P.Z. Zhang, H.A. Davies, R.A. Buckley, W.M. Rainforth, J. Magn. Magn. Mater. 128 (1993) 307.
[11] A. Manaf, R.A. Buckley, H.A. Davies, J. Magn. Magn. Mater. 128 (1993) 302.
[12] A. Manaf, P.Z. Zhang, I. Ahmad, H.A. Davies, R.A. Buckley, IEEE Trans. Magn. 29 (6) (1993) 2866.
[13] J. Bauer, M. Seeger, A. Zern, H. Kronmüller, J. Appl. Phys. 80 (3) (1996) 1667.
[14] G.C. Hadjipanayis, W. Gong, J. Appl. Phys. 64 (1988) 5559.
[15] T. Schrefl, J. Fidler, H. Kronmüller, Phys. Rev. B 49 (1994) 6100.
[16] R. Skomski, J.M.D. Coey, Phys. Rev. B 48 (1993) 15812.
[17] R. Coehoorn, D. de Waard, J. Magn. Magn. Mater. 83 (1990) 228.
[18] S. Hirosawa, H. Kanekiyo, M. Uehara, J. Appl. Phys. 73 (10) (1993) 6488.
[19] H. Kanekiyo, M. Uehara, S. Hirosawa, IEEE Trans. Magn. 29 (6) (1993) 2863.
[20] S. Hirosawa, H. Kanekiyo, 13th International Workshop on RE Magnets their Applications, 1994, p. 87.
[21] M. Uehara, T.J. Konno, H. Kanekiyo, S. Hirosawa, K. Sumiyama, K. Suzuki, J. Magn. Magn. Mater. 177–181 (1998) 997.
[22] J. Wecker, H. Cerva, C. Kuhrt, L. Schultz, J. Appl. Phys. 76 (1994) 6238.
[23] L. Schultz, K. Schnitzke, J. Wecker, M. Katter, C. Kuhrt, J. Appl. Phys. 70 (1991) 6339.
[24] T. Schrefl, J. Fidler, MRS Spring 99 meeting, Proceedings Symposium I, April 5–9, 1999.
[25] T. Schrefl, J. Fidler, IEEE Trans Magn. (1999) Intermag 99 paper FA-01, in press.
[26] J. Fidler, T. Schrefl, Proceedings of the X Symposium on Magnetic Anisotropy and Coercivity in RE–TM alloys, Dresden, Werkstoff-Informationsges., Frankfurt, 1998, p. 267.
[27] J. Fidler, J. Bernardi, T. Schrefl, Scripta Metall. 33 (10-11) (1995) 1781.
[28] J. Bernardi, G.F. Soto, J. Fidler, S. David, D. Givord, J. Appl. Phys. 85 (8) (1999) 5905.